

PROPOSITION OF A UNIFIED MODEL TO PREDICT STRENGTH AND FATIGUE LIFETIME OF 3D WOVEN COMPOSITE STRUCTURES WITH POLYMER MATRIX

F. Laurin¹, M. Kaminski¹, L. Angrand² and R. Desmorat³

¹ONERA, DMAS, Université Paris-Saclay, F-92322 Châtillon, France

Email : frederic.laurin@onera.fr, myriam.kaminski@onera.fr, Web Page: <http://www.onera.fr>

²Safran Aircraft Engines, F-77550 Moissy Cramayel, France

Email : lise.angrand@safrangroup.com, Web Page: <http://www.safran-group.com>

³LMT, ENS Paris-Saclay/CNRS/Université Paris-Saclay, F-94235 Cachan, France

Email : desmorat@lmt.ens-cachan.fr, Web Page: <http://lmt.ens-paris-saclay.fr>

Keywords: 3D woven composite; damage model; fatigue lifetime; finite element simulations

Abstract

A unified damage and failure approach has been proposed to estimate the failure of 3D woven composite materials subjected to static and/or fatigue loadings. Indeed, the existing damage and failure approach developed by Onera for static loading has been extended in the present paper to predict the damage evolution during fatigue loading, even for multiaxial spectral loadings, using an incremental damage formalism. The fatigue lifetime predictions, the evolution of apparent modulus and S-N curves for different stress ratios, have been compared successfully with the available tests carried-out by Safran Group. Moreover, this unified approach has been implemented into a commercial finite element code and applied successfully to different composite structures subjected to fatigue loading.

1. Introduction

The use of composite materials in both civil and military aeronautic applications keeps on increasing from the last decades thanks to its interesting specific rigidity and strength but classical laminated solutions are very sensitive to delamination occurring after impact. Therefore, 3D woven composite materials have been developed to obtain higher out-of-plane mechanical properties (rigidity and strength) and interesting residual properties after impact. Safran Aircraft Engines has thus chosen such a material for the manufacturing of the fan blades of its new generation of civil engine. Moreover, due to the imperative of structural mass reduction and consumption minimization for recent airliners, structures are subjected, during in-life service, to higher loadings for longer durations. Consequently, a robust methodology to predict the strength and the lifetime of industrial composite components subjected to real complex multiaxial loadings is needed. Among the different existing fatigue lifetime prediction methods [1], progressive fatigue damage models are the most promising for composites. Therefore, in the present paper, a unified damage and failure approach is proposed to predict the failure of 3D woven composite structures subjected to static and/or fatigue loadings.

In section 2.1, the damage mechanisms encountered during static and fatigue loadings in 3D woven composite materials are firstly detailed. In section 2.2, the damage and failure model, already developed at Onera [2] which allows describing accurately the different damage mechanisms encountered in 3D woven composites under static loading, is firstly briefly reminded. Then, this model has been extended to predict the fatigue lifetime based on an incremental formalism [3,4], which is able to predict the damage evolution during fatigue loading even for multiaxial spectral loadings. In section 3.1, the identification procedure of such a model is described and applied on the available test results. Finally, in section 3.2, the predictions of the present approach on other test configurations are compared successfully with the available test results. Finally, in section 4, the present approach is

applied on different composite structures, with an increasing complexity, in order to demonstrate its transferability to a design office in aeronautical industries.

2. Proposition of a unified damage and failure model

2.1. Damage mechanisms encountered in 3D woven composite materials

The architecture of 3D woven composite materials has been designed in order to avoid large delamination and to obtain only diffuse damage within the material. In the present study, an unbalanced 3D woven architecture is considered using carbon fibres embedded in an epoxy resin.

The damage mechanisms, observed during a static tensile test in the warp direction [2], are diffuse and located in the resin pockets between the fibre yarns. The damage orientation is piloted by the microstructure due to the contrast between the elementary constituents. The final failure is due to rupture of the warp fibre yarns in tension. During fatigue tensile tests in the warp direction, with a stress ratio close to 0, the same diffuse damage mechanisms are observed [5]. Therefore, it is relevant to assume that the damage, observed during static and fatigue loadings, presents the same effects on the behaviour. Moreover, the damage saturation value, linked to the microstructure, is also equivalent. Nevertheless, the damage evolution laws are different. Indeed, the damage evolution during fatigue loadings is highly slower than that observed during static loadings. In the present approach, it is thus assumed that a distinction can be made between the evolution damage law for static loadings and for fatigue, as proposed in [4]. Finally, the final failure is again due to the rupture of the fibre yarns in tension, but the strain at failure is lower than for static loading, meaning that assuming a coupling between the damage state and the apparent strain at failure for such a material is relevant.

2.2. Macroscopic damage model

The Onera Damage Model for Composites with Polymer Matrix (ODM-PMC) is based on continuum damage approaches defined at the macroscopic scale [2], in order to be used in design office for the strength predictions of composite structures representative of some industrial problematic. For the considered composite material with polymer matrix, it is assumed that the observed non-linearities are only due to the damage and failure mechanisms. Considering the different damage mechanisms, the ODM-PMC model considers 3 matrix scalar damage variables, which are (i) the damage in the warp direction noted d_1 , (ii) the damage in the weft direction noted d_2 and (iii) the yarn/matrix debondings in the out-of-plane direction noted d_3 . It can be noted that the influence of the viscosity of the matrix on the macroscopic behaviour has been neglected here for the sake of simplicity but should be considered in future works.

The present approach is thermodynamically consistent and thus the macroscopic behaviour, expressed in Eq. 1, derives directly from the Helmholtz free energy.

$$\underline{\underline{\sigma}} = \underline{\underline{C}}^{eff} : \underline{\underline{\varepsilon}} \quad \text{with} \quad \underline{\underline{C}}^{eff} = \left(\underline{\underline{S}}^0 + \sum_i d_i \underline{\underline{H}}_i \right)^{-1} \quad \text{and} \quad i = \{1,2,3\} \quad (1)$$

where $\underline{\underline{\sigma}}$ is the stress tensor, $\underline{\underline{C}}^{eff}$ is the effective elastic stiffness tensor taking into account the effects of the different damage mechanisms and $\underline{\underline{\varepsilon}}$ the total strain tensor. In the present approach, the effects of damage mechanisms (yarn/matrix debondings, transverse cracking in the matrix ...) on the macroscopic behaviour are considered in the ODM-PMC by increasing the initial elastic compliance $\underline{\underline{S}}^0$ with a term describing the effects of matrix damages ($\sum d_i \underline{\underline{H}}_i$) which depends on the damage variables d_i and the corresponding effect tensors $\underline{\underline{H}}_i$, describing the effects of an open crack on the effective stiffness.

The driving forces associated to the different damage variables are expressed in Eq. 2 and depend on (i) the different components of the initial elastic stiffness tensor, (ii) on the parameters (a_{15} , a_{16} , a_{24} , a_{26} , a_{34} , a_{35}) which are material coefficients linked to the onset of damage under shear loadings and (iii) on the positive strain tensor. The positive strain tensor, associated to a driving force, corresponds to the positive part of the total strain tensor where all the components are zeros except those inducing damages and reported in Eq. 2. The use of the positive strain tensor is an elegant way to capture the reinforcement of the apparent onset of damage for combined compressive and shear loadings, as demonstrated experimentally [2], without introducing additional coefficients. Moreover, the equivalent strains have been defined, as a function of the driving forces, to be homogeneous to a strain in order to be easily used in a design office of aeronautical industries.

$$\begin{cases} y_1 = \frac{1}{2} \left(C_{11}^0 \varepsilon_1^{1+2} + a_{15} C_{55}^0 \varepsilon_5^{1+2} + a_{16} C_{66}^0 \varepsilon_6^{1+2} \right) \\ y_2 = \frac{1}{2} \left(C_{22}^0 \varepsilon_2^{2+2} + a_{24} C_{44}^0 \varepsilon_4^{2+2} + a_{26} C_{66}^0 \varepsilon_6^{2+2} \right) \\ y_3 = \frac{1}{2} \left(C_{33}^0 \varepsilon_3^{3+2} + a_{34} C_{44}^0 \varepsilon_4^{3+2} + a_{35} C_{55}^0 \varepsilon_5^{3+2} \right) \end{cases} \quad \text{and} \quad \begin{cases} \varepsilon_{eq(1)} = \sqrt{\frac{2 y_1}{C_{11}^0}} \\ \varepsilon_{eq(2)} = \sqrt{\frac{2 y_2}{C_{22}^0}} \\ \varepsilon_{eq(3)} = \sqrt{\frac{2 y_3}{C_{33}^0}} \end{cases} \quad (2)$$

Concerning the effects of the different damage mechanisms, in the warp direction for instance, the effect tensor $\underline{\underline{H}}_1$ associated to the damage variable d_1 is defined as a function of a deactivation index (η_1) and of an effect tensor ($\underline{\underline{H}}_1^+$) describing the effects of an open crack on the effective elastic stiffness, as reported in Eq. 3. The parameters (h_{11}^{m+} , h_{55}^{m+} , h_{66}^{m+}) are material coefficients.

$$\underline{\underline{H}}_1 = \eta_1 \underline{\underline{H}}_1^+ \quad \text{with} \quad \begin{cases} \eta_1 = \begin{cases} 1 & \text{if } \sigma_{11}^\eta \geq 0 \\ 0 & \text{instead} \end{cases} \\ \text{and } \underline{\underline{\sigma}}^\eta = \underline{\underline{C}}^{eff} : \underline{\underline{\varepsilon}} \end{cases} \quad \text{and} \quad \underline{\underline{H}}_1^+ = \begin{pmatrix} h_{11}^{m+} S_{11}^0 & 0 & 0 & 0 & 0 & 0 \\ & 0 & 0 & 0 & 0 & 0 \\ & & 0 & 0 & 0 & 0 \\ & & & 0 & 0 & 0 \\ sym. & & & h_{55}^{m+} S_{55}^0 & 0 \\ & & & & h_{66}^{m+} S_{66}^0 \end{pmatrix} \quad (3)$$

A special attention has been paid to the unilateral aspect of damage (and thus to the activation index) in order to avoid discontinuity for complex non proportional multiaxial loadings. The cracks are assumed closed (meaning $\eta_1 = 0$) when the component 11 of the effective stress ($\underline{\underline{\sigma}}^\eta$) is strictly inferior to zero and opened otherwise (meaning $\eta_1 = 1$). The effect tensors and the associated activation indexes for the other damage variables can be obtained thanks to permutation of the indices.

The damage evolution law is the key point of the present incremental damage approach and is based on [4,2]. Indeed, the damage rate law can be decomposed in two parts: (i) the damage evolution generated during the static loading and (ii) the damage evolution during fatigue, as reported in Eq. 4; which cannot be activated at the same time. For static loadings, the maximal equivalent strain during the loading increases as the current equivalent strain. Therefore, only the first term of the Eq. 4 is activated. The ($S_{m(k)}^k, s_m^k, \varepsilon_{0(k)}^m$) parameters are materials coefficients. It can be noted that this formulation is strictly equivalent to that proposed in the previous static version of the model [2], avoiding thus to re-identify some parameters. For cyclic fatigue loadings, the maximal equivalent strain remains constant. Therefore, only the second term of the Eq. 4 is activated and induces the

damage evolution for fatigue loading. The parameter ($d_{\infty(k)}$) corresponds to the saturation of the damage which is currently observed for composites subjected to fatigue loading, ($\varepsilon_{0(k)}^f$) corresponds to the onset of fatigue damage and ($S_{f(k)}, s_f^k$) are material parameters linked to the evolution fatigue damage law. The present formulation allows only the damage growing during the loading phase. Moreover, the use of the equivalent strain is convenient even for complex multiaxial loadings.

$$\begin{aligned} \dot{d}_k &= (d_{\infty(k)} - d_k) \left\langle \frac{\varepsilon_{eq(k)}^{\max} - \varepsilon_{0(k)}^m}{S_{m(k)}} \right\rangle_+^{s_m^k} \left\langle \dot{\varepsilon}_{eq(k)}^{\max} \right\rangle_+ \\ &+ (d_{\infty(k)} - d_k)^{\gamma_k} \left\langle \frac{\varepsilon_{eq(k)} - m_k \tilde{\varepsilon}_{eq(k)} - \varepsilon_{0(k)}^f}{S_{f(k)}} \right\rangle_+^{s_f^k} \left[\left\langle \dot{\varepsilon}_{eq(k)} \right\rangle_+ - \dot{\varepsilon}_{eq(k)}^{\max} \right] \end{aligned} \quad (4)$$

with $\varepsilon_{eq(k)}^{\max} = \sup_{t \leq \tau} [\varepsilon_{eq(k)}(t)]$ and $\tilde{\varepsilon}_{eq(k)} = \frac{I_{(k)}}{Z_{ac(k)}}$ avec $\begin{cases} I_{(k)} = \int \varepsilon_{eq(k)} |d\varepsilon_{eq(k)}| \\ Z_{ac(k)} = \int |d\varepsilon_{eq(k)}| \end{cases}$

Moreover, it has been demonstrated that it is an absolute necessity to introduce the influence of the average equivalent strain ($\tilde{\varepsilon}_{eq(k)}$) in the damage evolution law (reported in Eq. 4) in order to be able to describe the evolution of the S-N curves as a function of the stress ratios. The influence of the average equivalent strain can be calibrated thanks to the material parameter (m_k). The average quantity has been formulated in order (i) to be insensitive to the number of loading increments, (ii) to be insensitive to the shape of cycles and (iii) to tend to the average quantity for a cyclic loading (*i.e.* $\lim_{t \rightarrow +\infty} \tilde{\varepsilon}_{eq(k)}(t) = 0.5(\varepsilon_{eq(k)}^{\max} + \varepsilon_{eq(k)}^{\min})$). These three conditions are essential in order to use such an approach in finite element simulations for structures subjected to complex loadings.

2.3. Final failure criteria

The final failure of the specimens are due to fibre yarn failures in the warp and weft directions in tension (f_1^t, f_2^t) or in compression (f_1^c, f_2^c). In the previous version of the model, the failure criteria used for the failure of the fibre yarns are simple maximal strain criteria in the warp and weft directions. Moreover, the failure in tension and in compression is distinguished because the involved failure mechanisms are very different. As proposed in the literature [6], it has been demonstrated that the effective strain at failure in tension must be defined as a function of the damage state in order to predict accurately the fatigue lifetime of composite material, as reported in Eq. 5. For static/fatigue tensile loadings in the warp direction (*i.e.* positive stress ratio evolving between 0 and 1), the parameters ($\varepsilon_{11}^{Rt}, d_1^R$) (and ($\varepsilon_{22}^{Rt}, d_2^R$) in the weft direction) must be identified using two different tests in which the damage states at failure are different, such as a static test and a fatigue test (for instance at a high given percentage of the failure stress). The coupling between the damage and the compressive strain at failure has not been yet investigated because of the difficulty to perform accurate fatigue tests. This point will be under consideration soon.

$$\left\{ \begin{array}{l} f_1^t = \frac{\varepsilon_{11}}{\tilde{\varepsilon}_{11}^{Rt}} \text{ with } \tilde{\varepsilon}_{11}^{Rt} = \varepsilon_{11}^{Rt} \cdot \left\langle \frac{d_1^R - d_1}{d_1^R} \right\rangle_+ \\ f_2^t = \frac{\varepsilon_{22}}{\tilde{\varepsilon}_{22}^{Rt}} \text{ with } \tilde{\varepsilon}_{22}^{Rt} = \varepsilon_{22}^{Rt} \cdot \left\langle \frac{d_2^R - d_2}{d_2^R} \right\rangle_+ \end{array} \right\} \text{ and } \left\{ \begin{array}{l} f_1^c = \frac{\varepsilon_{11}}{\tilde{\varepsilon}_{11}^{Rc}} \text{ with } \tilde{\varepsilon}_{11}^{Rc} = \varepsilon_{11}^{Rc} \cdot \left\langle \frac{d_3^R - d_3}{d_3^R} \right\rangle_+ \\ f_2^c = \frac{\varepsilon_{22}}{\tilde{\varepsilon}_{22}^{Rc}} \text{ with } \tilde{\varepsilon}_{22}^{Rc} = \varepsilon_{22}^{Rc} \cdot \left\langle \frac{d_3^R - d_3}{d_3^R} \right\rangle_+ \end{array} \right\} \quad (5)$$

To conclude, the present approach is able to predict both the evolution of the effective Young modulus of a 3D woven composite material subjected to static/fatigue loading and the strength or the fatigue lifetime of such a material subjected to cyclic fatigue loading, even for real complex spectral loadings.

3. Identification and validation of the present model

3.1. Identification procedure

In order to transfer such an approach to a design office, it is necessary to propose a clear identification procedure. For the present model applied to a given orthotropic 3D woven composite material, 7 different tests are needed: (i) one static tensile test at failure in the warp (and weft) direction, (ii) two fatigue tests at failure in the warp (and weft) direction with a fixed stress ratio (close to 0) and with two different maximal stresses and (iii) an off-axis tensile tests at failure at 45° (for influence of damage on the in-plane shear modulus). It can be noted that the compressive and the out-of-plane parts of the model are not considered in the present study but should be in future works.

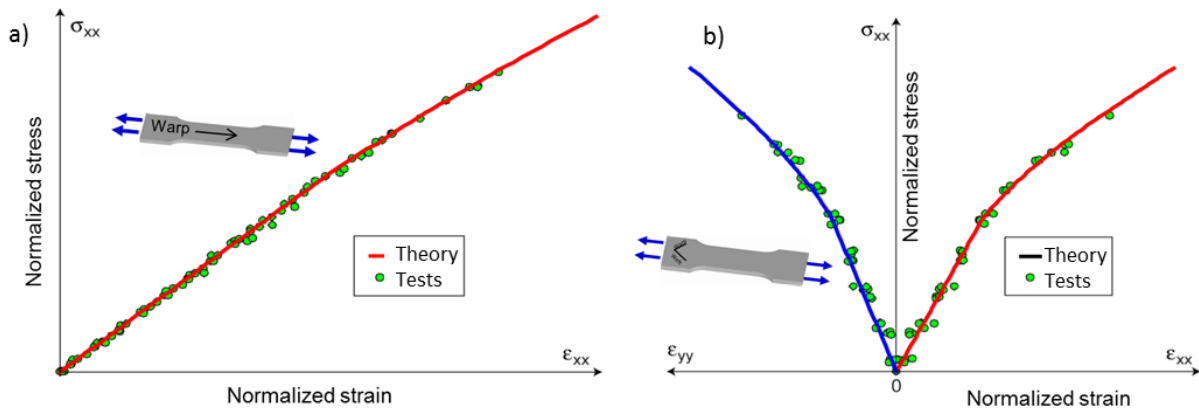


Figure 1. Comparisons between the normalized experimental strain/stress curves and the predictions obtained with ODM-PMC for (a) a tensile test at 0° and (b) an off-axis tensile tests at 45°.

For all these tests, it is an absolute necessity to measure the evolution of the strain during the static and the fatigue loadings using an extensometer (real one or a virtual one using the strain field measured with digital image correlations). Indeed, the strain is used to estimate both the evolution of the apparent modulus (to identify the parameters linked to the damage evolution) and the strain at failure for static tests and also for cyclic fatigue loadings (to identify the coupling between the damage and the apparent strain at failure).

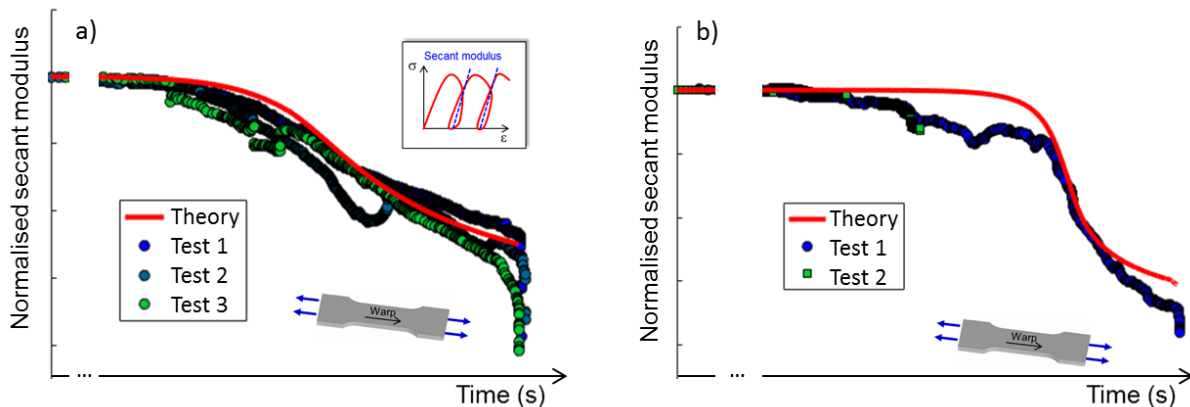


Figure 2. Comparisons between the experimental modulus and the estimations obtained with ODM-PMC for fatigue tensile tests (a) at 60% and (b) 40% σ_r in the warp direction, $R_\sigma \approx 0$ at 5 Hz.

It can be noted that the most difficult point in the identification process is linked to the identification of the onset of damage for fatigue loading, which is linked to the fatigue limit of the material. This point could be achieved using the asymptotic part of S-N curves (method used in the present study) or using self-healing method recently developed for composite materials [7].

Fig. 1 presents the comparisons between the normalized estimated macroscopic stress/strain and the measurements performed at Onera on static tensile tests at 0° and 45° [2]. Moreover, Fig. 2 presents the comparisons between the normalized estimated apparent modulus and the measurements for two fatigue tests with a stress ratio close to 0 and with two different maximal stresses in the warp direction. It has also been performed in the weft direction. The present approach is thus able to describe in a very accurate manner the static and fatigue tests which have been used during the identification procedure considering both the evolution of the apparent modulus and the failure or the fatigue lifetime during cyclic loading.

3.2. Validation of the present approach

In this section, the predictive capabilities of the unified damage and failure approach are evaluated through the comparisons with available test results which have not been used during the identification process.

Considering the validation of the damage evolution during fatigue loading, Fig. 3 presents the comparisons between the predicted evolution of the apparent modulus and the measurements on fatigue tests performed with $R_\sigma \approx 0$ at 5 Hz and with different maximal stresses, defined as a percentage of the stress at static failure. The predictions are in good agreement with the available experimental data. The same accuracy is obtained in the weft direction.

For the prediction of the fatigue lifetime of 3D woven specimens, the S-N curves estimated with the present approach have been compared successfully with the available tests in the weft (see Fig. 5a) and warp directions (see Fig. 5b-d). It is reminded that the model has been identified for the failure part using only one static test and one fatigue test at failure. Moreover, it can be noted that the predicted S-N curves for different stress ratios (evolving between 0 and 1), reported in Fig. 5b-c, are in good agreement with test results, mainly thanks to the introduction of the average equivalent strain in the damage evolution (see Eq. 4).

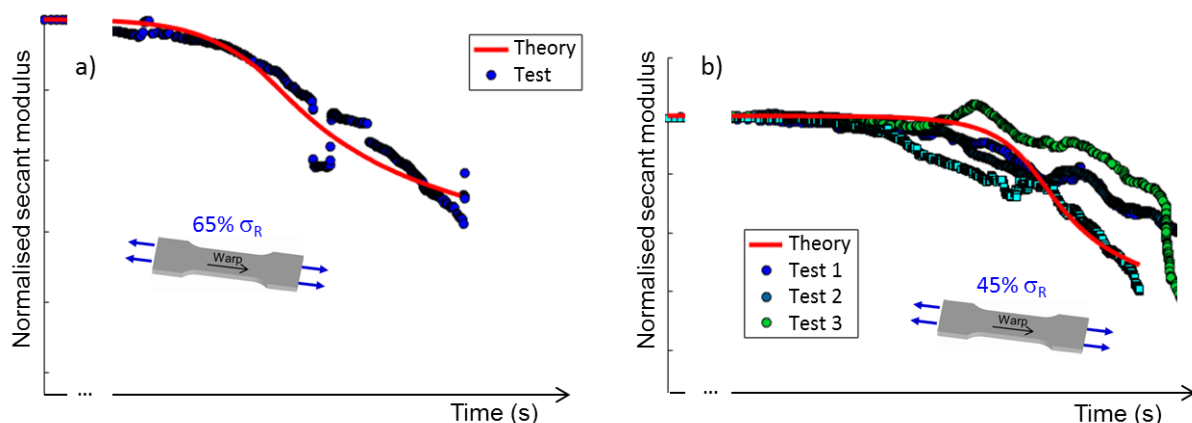


Figure 3. Comparisons between the experimental modulus and the predictions obtained with ODM-PMC for fatigue tensile tests (a) at 65% and (b) 45% σ_r in the warp direction, $R_\sigma \approx 0$ at 5 Hz.

Therefore, the fatigue lifetime predictions, meaning the evolution of the apparent modulus during fatigue loading and the prediction of S-N curves, even for different positive stress ratios, are in good agreement with the available tests carried-out by Safran.

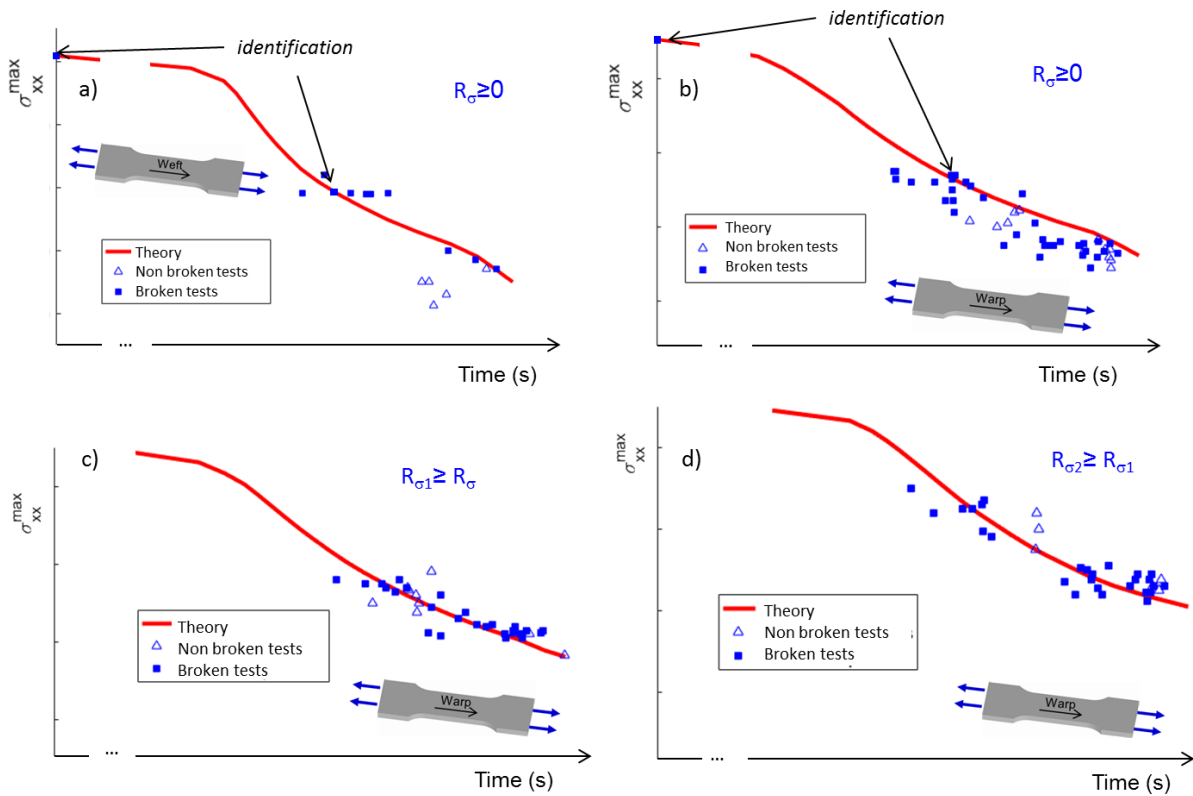


Figure 4. Comparisons between the predicted S-N curves with ODM-PMC and the test results in (a) the weft direction with $R_\sigma \approx 0$ at 5Hz and (b-d) in the warp direction for three increasing stress ratios ($0 \leq R_\sigma \leq R_{\sigma 1} \leq R_{\sigma 2}$) evolving between 0 and 1 at 5Hz.

4. First application to composite structures

Then, the present approach has been implemented in a commercial finite element code to estimate the damage evolution during static and fatigue loadings. A special attention has been paid to the computation of the consistent tangent matrix in order to reduce the computational time and increase the robustness of such a damage model. This model has been applied to different composite structures with an increasing complexity, starting on elementary cube to an open-hole plate or even bolted joints.

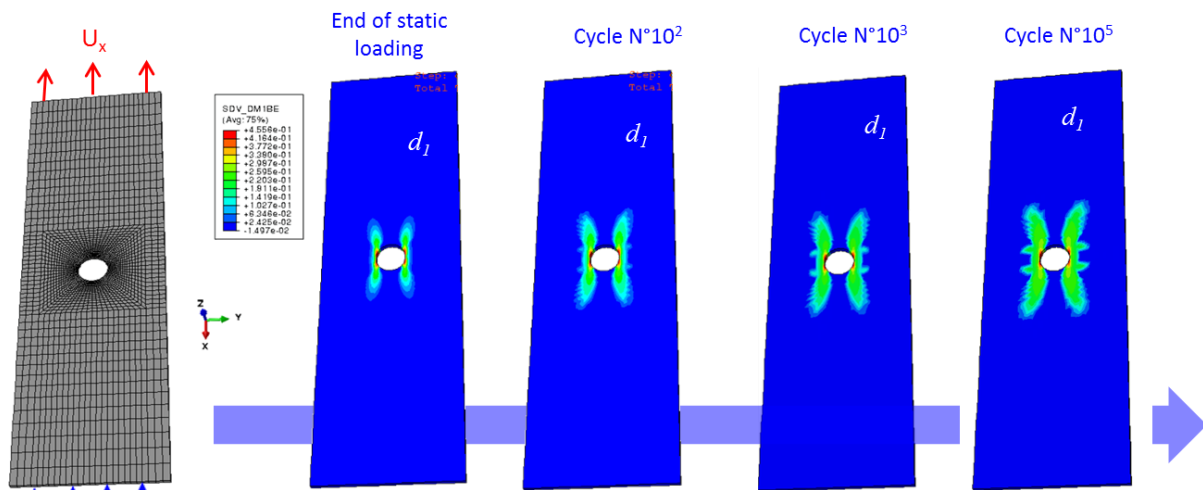


Figure 5. Predictions of the damage evolution in an open-hole plate subjected to fatigue loading during 10^5 cycles, at $U^{\max} = 0.4\text{mm}$, $R_u = 0$ and $f = 5\text{Hz}$.

In Fig. 5, the open-hole plate test case is described. The diameter of the hole is equal to 6.35mm and the ratio width of the plate over diameter of the hole is equal to 5. The warp direction of the material corresponds to the length of the specimen. A fatigue loading, piloted with displacement, has been applied with a displacement ratio equal to 0 with a frequency of 5 Hz. In order to demonstrate that the present approach could be applied to composite structure, 10^5 cycles have been simulated in 40 minutes, which is very promising without considering any computational strategy such as jump cycle method for instance [1]. The damage evolution during the different cycles seems to be relevant and will be compared soon with test results currently performed at Onera.

5. Conclusions and perspectives

A damage and failure approach has been proposed for 3D woven composite materials with polymer matrix in order to predict the strength and the fatigue lifetime of composite parts subjected to real complex loadings. Based on the existing continuum damage model, ODM-PMC, developed to predict the strength of composite structures subjected to static loading, an extension has been proposed in this study to predict the damage evolution during fatigue loadings, using an incremental damage formalism. The choice of such a formalism has been performed in order to consider even complex spectral fatigue loadings, representative of those encountered in real composite components. An identification procedure has been proposed and applied to the available test results. Then, the predictions obtained with the present approach, in terms of damage evolution and fatigue lifetime during cyclic fatigue loadings, are in good agreement with the available experimental data, even for different stress ratios. Finally, this model has been implemented in a commercial finite code and applied successfully to different structures with reasonable computational times. Future works will consist in performing comparisons between the strength and fatigue lifetime predictions obtained on composite structures with test results, currently performed at Onera.

Acknowledgements

The collaboration with SAFRAN Ceramics is gratefully acknowledged. This work was supported under PRC MECACOMP, French research project co-funded by DGAC and SAFRAN Group, piloted by SAFRAN Group and involving SAFRAN Group, ONERA and CNRS.

References

- [1] W. Van Paepegem and J. Degrieck, Fatigue degradation modelling of plain woven glass/epoxy composites, *Composites Part A: Applied Science and Manufacturing*, 32 (10): 1433-1441, 2001.
- [2] C. Rakotoarisoa. Pr evision de la dur ee de vie en fatigue des composites   matrice organique tiss es interlock. *Doctorate thesis of Universit  de Technologie de Compi gne*, 2014.
- [3] L. Angrand. Mod le d'endommagement incr mental en temps pour la pr vision de la dur ee de vie des composites tiss s 3D en fatigue cyclique et en fatigue al atoire. *Doctorate thesis of Universit  Paris-Saclay*, 2016.
- [4] J. Lemaitre, R. Desmorat, M. Sauzay, Loi d' volution de l'endommagement anisotrope, *Comptes Rendus de l'Acad mie des Sciences - Series IIB - Mechanics-Physics-Astronomy*, 327 (12): 1231-1236, 1999.
- [5] J. Henry. Etude et analyse des m canismes d'endommagements en fatigue des composites   renforts tissus interlocks. *Doctorate thesis of Universit  de Technologie de Compi gne*, 2013.
- [6] D. Caous, R le de l'endommagement sur la dur ee de vie en fatigue des mat riaux composites stratifi s : application au domaine  olien, *Doctorate thesis of  cole Nationale Sup rieure d'Arts et M tiers*, 2017.
- [7] L. M ller, J.-M. Roche, A. Hurmane, C. Peyrac and L. Gornet. Accelerated estimation of fatigue performances of thermoplastic composite materials by self-heating monitoring. *Proceedings of the 18th European Conference on Composite Materials ECCM-18, Athens, Greece, June 24-28 2018*.